Environmental Science and Pollution Research (2019) 26:25609–25620
https://doi.org/10.1007/s11356-019-05832-5

RESEARCH ARTICLE

Solidification/stabilization of municipal solid waste incineration fly ash using uncalcined coal gangue–based alkali-activated cementitious materials

Shujie Zhao[1,2] · **Faheem Muhammad**[1,2] · **Lin Yu**[2] · **Ming Xia**[1,2] · **Xiao Huang**[1,2] · **Binquan Jiao**[1,2] · **Ning Lu**[3] · **Dongwei Li**[1,2]

Received: 25 March 2019 / Accepted: 24 June 2019 / Published online: 2 July 2019

Abstract

The proper disposal of municipal solid waste incineration fly ash (MSWI FA) is necessary due to the presence of hazardous metals (Cu^{2+}, Zn^{2+}, Pb^{2+} and Cd^{2+}). The solidification/stabilization through alkali-activated cementitious materials (having aluminosilicates) is regarded as one of the best methods for its disposal. In this paper, an uncalcined coal gangue–based alkali-activated cementitious material was used to solidify the MSWI FA. The compressive strength of these cementitious materials was evaluated through different contents of alkali activators, SiO_2/Na_2O molar ratios, liquid/solid ratios and curing temperatures by utilizing a single-factor experiment. The specimens with the highest compressive strength (31.37 MPa) were used for solidification of MSWI FA. The results indicated that compressive strength decreased with the addition of MSWI FA which caused the higher leaching of heavy metals. The solidification efficiencies of Cu^{2+}, Zn^{2+}, Pb^{2+} and Cd^{2+} were more than 95%. In addition, leaching concentrations had not surpassed the critical limit up to 20% addition of MSWI FA in solidified samples and representing the potential application of these samples for construction and landfill purposes. Heavy metals in MSWI FA were solidified through physical encapsulation and chemical bonding which was verified by speciation analysis, X-ray diffraction, Fourier transform infrared spectrometry and scanning electron microscopy with energy dispersive spectrometry analyses.

Keywords MSWI fly ash · Uncalcined coal gangue · Solidification · Compressive strength · Alkali-activated material · Heavy metals

---

Shujie Zhao, Faheem Muhammad, Lin Yu and Ming Xia contributed equally to this work.

Highlights

- The coal gangue without calcination is used for the preparation of alkali-activated cementitious materials.
- Uncalcined coal gangue has potential to solidify the MSWI FA.
- Solidified bodies could also be used as construction materials and landfill disposal.

Responsible editor: Bingcai Pan

✉ Xiao Huang
shawwong@126.com

✉ Binquan Jiao
j.binquan@cqu.edu.cn

✉ Ning Lu
cqsft_lu@163.com

✉ Dongwei Li
litonwei@cqu.edu.cn

[1] State Key Laboratory for coal mine disaster dynamics and control, Chongqing University, Chongqing 400044, People's Republic of China

[2] College of Resource and Environmental Science, Chongqing University, Chongqing 400044, China

[3] College of Safety Engineering, Chongqing University of Science and Technology, Chongqing 400044, China

Introduction

Rapid industrialization and urbanization have resulted in an increase of various industrial solid wastes, e.g. municipal solid waste incineration fly ash (MSWI FA) and coal gangue (CG). The presence of toxic heavy metals, furans and dioxins in MSWI FA makes it toxic waste. According to an estimation, more than 4 million tons of MSWI FA in China has been generated in 2016 (Du et al. 2018; Yue et al. 2019). Another problem associated with MSWI FA is its random stacking in the form of heaps has occupied a large volume of land. Therefore, it is need of time to address these problems properly which can limit the leaching of heavy metals from these heaps and save the land.

In the past, several technologies have been carried out for the treatment of hazardous wastes, but solidification/stabilization is considered as the best available technology because of its effectiveness for almost 57 kinds of different wastes (Muhammad et al. 2018). Ordinary Portland cement (OPC) was widely used as a solidifying agent (Chen et al. 2019; Wang et al. 2019a, 2018a). Nevertheless, OPC has several disadvantages including low mechanical strength, high consumption of energy along with input resources and high emission of CO_2. Hence, the high investigational value regarding the development of new solidification/stabilization materials which have superior properties and have a good market outlook is required.

The AAM is an inorganic polymer, which is formed by the reaction of source materials (rich in aluminosilicates, e.g. industrial by-products, natural minerals or wastes) with an alkali activator (Benito et al. 2013). Several common raw materials are used for the synthesis of AAM such as coal fly ash (Giasuddin et al. 2013), blast furnace slag (Kumar et al. 2019) and calcined clays (e.g. metakaolin) (Pelisser et al. 2013). Generally, the geopolymerization process or alkali activation process proceeds in the following order: (i) dissolution, the source material is dissolved into its precursors, i.e. aluminium and silicon upon reaction with a strong alkaline solution; (ii) recombination and replacement among dissolved ions; (iii) gelation, C-(A)-S-H and N-A-S-(H) gels are formed; (vi) solidification and strengthening of gels; (v) continuous formation of gel results in crystallization (Reig et al. 2013). In comparison with OPC, the superior properties (eco-friendly, good mechanical properties, high resistance against corrosion and temperature, etc.) of AAM are more favourable for solidification of toxic heavy metals (Istuque et al. 2019; Moukannaa et al. 2019).

The solidification efficiency of geopolymer/AAM regarding waste stabilization/toxic metals is measured through mechanical properties and the leaching process, while the leaching process and strength have an inverse relation (Bie et al. 2016; Pereira et al. 2009). The final properties such as mechanical properties of AAM are influenced by several factors which include source material, alkali activator ratio, water content, curing temperature, nature and concentration of wastes. The effect of these factors on compressive strength was studied by Muhammad et al. (2018) and they had verified the previous statement. Komnitsas et al. (2015) had found maximum compressive strength at 10 M concentrations of NaOH after utilizing four different concentrations (8, 10, 12 and 14 M). According to them, its higher concentration remains unreacted because of the increase in residual concentration, while the lower concentration of NaOH cannot provide the required alkalinity in geopolymer binder. Therefore, lower and higher concentrations of NaOH resulted in a decrease in strength. Regarding the SiO_2/Na_2O ratio, Gao et al. (2014) had found that a higher compressive strength was attained by using the SiO_2/Na_2O ratio of 1.50. They had explained that the lower ratio of SiO_2/Na_2O resulted in the inhibition of dissolution of aluminosilicates and its higher ratio had a negative effect on the workability of geopolymer paste which inhibits the geopolymerization process. Hence, strength decreased ultimately. Similarly, water content and curing regime are also crucial factors regarding the geopolymerization process and strength development (Aredes et al. 2015; Zuhua et al. 2009).

A number of scientists had immobilized various kinds of wastes in geopolymer/AAM (Hu et al. 2018; Lee et al. 2016; Santa et al. 2016; Wang et al. 2019b; Ye et al. 2016). Muhammad et al. (2018) had found that a reasonable range of Pb^{2+}, Cr^{6+} and Cd^{2+} could be effectively immobilized in the geopolymer matrix through chemical and physical ways and the addition of these metals had affected the geopolymer structure (compressive strength) to varying degrees. Lee et al. (2016) had studied the immobilization efficiency and mechanism of Pb^{2+} ions in fly ash–based cementitious materials and found that compressive strength decreased with the incorporation of Pb^{2+}. Besides, they also found that immobilization efficiency was largely dependent on the Si/Al ratio of geopolymer because large numbers of Al^{3+} species give rise to a negative charge which favours the immobilization of Pb^{2+} cations. Furthermore, Diaz-Loya et al. (2012) had solidified the MSWI FA by using AAM (coal fly ash–based geopolymer). They observed that the leaching concentration of heavy metals did not surpass the safe limits and the mechanical properties of solidified bodies (containing 60% of MSWI FA) were suitable for construction applications. These studies showed that AAM has momentous potential to immobilize various kinds of wastes including MSWI FA which has toxic metals including Cu^{2+}, Zn^{2+}, Pb^{2+} and Cd^{2+}.

CG is a solid waste which is a by-product of coal mine industries. According to an estimation, CG has been the top industrial solid waste in China with a total production of 4.5–5.0 billion tons (Deng et al. 2017; Dong 2018; Huang et al. 2018). The piling up of CG will not only occupy a large amount of land but also cause natural disasters such as landslides and mudslides. Recently, cementitious materials prepared with CG have been widely used in building construction. Basically, CG has fairly stable crystal structures including kaolinite and quartz which limit the cementitious activity. Therefore, CG is subjected to calcination at a higher temperature (> 600 °C) to improve its cementitious activity and it is used for the preparation of AAM (Liu et al. 2013; Zhang et al. 2011). However, this process (calcination) consumes a lot of heat energy likewise OPC. In order to save the heat energy, uncalcined CG was utilized for the preparation of AAM and then it was used for solidification of MSWI FA to limit the leaching of heavy metals.

In the present study, uncalcined CG was subjected for preparation of geopolymer/AAM and solidification of MSWI FA. The compressive strength of pure solidified AAM (without the addition of MSWI FA) was investigated by using different ratios of alkali contents, SiO_2/Na_2O molar ratios, liquid-to-solid (L/S) ratios and curing temperatures via a single-factor experiment. The specimen with the highest compressive strength was used for solidification of MSWI FA. In addition, the characteristic and solidification mechanism of CG-based cementitious materials were analysed by X-ray diffraction (XRD), Fourier transform infrared spectroscopy (FTIR) and scanning electron microscopy with energy dispersive spectrometry (SEM-EDS).

Materials and methods

Materials

The CG used in this experiment was brought from Shuozhou, Shanxi Province, China. It was sieved through a 325-mesh sieve after drying (105 °C) and milling/grinding for 12 h. The MSWI FA was obtained from a waste incineration power plant situated in Chongqing, China (incineration unit ≥ 950 °C). It was also dried at 105 °C and sieved through a 200-mesh sieve (75 μm) after 3 h of ball milling. Alkali activators were synthesized using analytical-grade sodium hydroxide (NaOH) and sodium silicate ($Na_2SiO_3 \cdot 9H_2O$). Deionized water was used throughout the experiment.

Experimental methods

Specimen preparation

The solidified bodies without MSWI FA were prepared by mixing and stirring the dried CG in activator solution for 10 min to make the dense paste. The moulds (20 mm × 20 mm × 20 mm) were filled with dense paste and placed in an oven under specified temperature (30, 45, 60, 75 or 90 °C). After 24 h, the samples were demoulded and cured for the specified time at room temperature. The specifications of different parameters in the single-factor experiment, i.e. alkali activator content, SiO_2/Na_2O molar ratio, L/S ratio and curing temperature are presented in Table 1. The purpose of studying various proportions of these parameters was to achieve the highest compressive strength.

Regarding the immobilization of waste, the different concentrations of MSWI FA (up to 60%) were substituted for CG (having highest compressive strength) on mass bases and solidified bodies were prepared as previously mentioned.

Compressive strength test

The compressive strength of the alkali-activated cementitious materials (AAM) was tested by AGN-250 universal testing machine (Shimadzu, Japan) after a specific time (7 and 28 days). The average compressive strength values of three replicates were used in the experiment.

Leaching test

Standard HJ/T 300-2007 (CN-HJ 2007) proposed by the State Environmental Protection Administration of China was used to evaluate the leaching toxicity of heavy metals from MSWI FA and solidified products containing MSWI FA. The specimens were crushed into granular material (< 9.5 mm) and subjected for leaching test. The leachate was prepared by the addition of 17.5 mL of CH_3CH_2OOH (to adjust the pH at 2.64 ± 0.05) in deionized water. The extraction solution with granular material was shaken for 18 h at 30 rpm and the liquid to solid ratio was 20. After filtration (with a 0.45-μm microporous filter), the heavy metal (Cu^{2+}, Zn^{2+}, Pb^{2+} and Cd^{2+}) concentration in the leaching solution was tested by using atomic absorption spectrometry as per GB 5085.3-2007 (CN-GB 2007). The evaluation of solidification efficiency was carried out by an immobilization ratio calculated by the following formula here.

$$\text{Immobilization ratio} = 1 - \frac{\text{Quality of each toxic heavy metal in the leaching solution}}{\text{Total mass of each toxic heavy metal in the initial solid}}$$

Characterization identification

X-ray fluorescence spectrometry (XRF, Shimadzu, Japan) was used to determine the chemical composition of CG and MSWI FA. The speciation analyses of each heavy metal of raw MSWI FA and the solidified bodies were performed by Tessier's sequential extraction method (Tessier et al. 1979). The structures and mineralogical compositions were measured by FTIR and XRD. The XRD patterns of specimens were determined by using X'Pert PRO (PANalytical B.V., Netherlands) with CuKα radiation at 2θ range from 5 to

Table 1 Single-factor experimental layout

ID	Alkali content (wt/%)	SiO_2/Na_2O molar ratio	L/S ratio	Temperature (°C)
A1	9	0.4	0.25	90
A2	12	0.4	0.25	90
A3	15	0.4	0.25	90
A4	18	0.4	0.25	90
A5	21	0.4	0.25	90
M1	15	0	0.27	90
M2	15	0.2	0.27	90
M3	15	0.4	0.27	90
M4	15	0.6	0.27	90
M5	15	0.8	0.27	90
L1	15	0.4	0.25	90
L2	15	0.4	0.27	90
L3	15	0.4	0.29	90
L4	15	0.4	0.31	90
L5	15	0.4	0.33	90
T1	15	0.4	0.27	30
T2	15	0.4	0.27	45
T3	15	0.4	0.27	60
T4	15	0.4	0.27	75
T5	15	0.4	0.27	90

90°. The samples (KBr pellets) were scanned with a FTIR spectrometer (Thermo Nicolet-5700, USA) within the range of 400–4000 cm^{-1}. The morphological characteristics of the specimens were analysed by SEM (VEGA3 TESCAN, Czech Republic) at an accelerated voltage of 15 kV. EDS was recorded with the same instrument.

Results and discussion

Characterization of raw materials

Before proceeding towards the further sections, it is necessary to discuss the compositional analysis of CG and MSWI FA which is presented in Tables 2 and 3. The CG was mainly composed of SiO_2 and Al_2O_3 which could be applied in the preparation of geopolymer/AAM, while Ca and O were dominant components of MSWI FA and chloride contents were approximately 11.95%. A large number of chlorides might have an adverse effect on the durability of solidified bodies. In addition, the major four heavy metals (Cu^{2+}, Zn^{2+}, Pb^{2+} and Cd^{2+}) with leaching risk in MSWI FA are presented in Table 3.

As demonstrated in Fig. 1, the leaching ratios of Cu^{2+}, Zn^{2+}, Pb^{2+} and Cd^{2+} of MSWI FA varied with initial pH of leaching solution variation. The significant decline in leaching concentration of heavy metals was observed with the increase in initial pH from 2.0 to 3.0. Taking Cu^{2+} as an example, its leaching rate decreased from 91.81 to 2.43% when the initial pH changed from 2.0 to 3.0. The decrease in leaching concentration might be due to the formation of insoluble hydroxides at high pH (Zhan et al. 2018), while the final pH increased sharply after the addition of MSWI FA in the leaching medium due to its high acid buffering capacity.

The solidification/stabilization efficiency would be affected if heavy metal ions precipitated as insoluble hydroxides. To mitigate this effect, leachate with low pH and high buffering capacity should be used in the leaching test. Thus, HJ/T 300-2007 method was used for leaching purposes.

Effect of different factors on strength

The effect of various factors on the compressive strength of CG–based cementitious materials was analysed by using a single-factor experiment. Additionally, the results of single-factor experiments are demonstrated in Fig. 2.

(a) Alkali contents

The unconfined compressive strengths of CG–based cementitious materials influenced by different alkali contents are shown in Fig. 2a. The compressive strength was increased with the addition of alkali content up to 12%. The increase in strength is attributed to the acceleration of the dissolution of aluminium and silicon precursors in the presence of OH^-, and the reaction of $[SiO_4]$ and $[AlO_4]$ tetrahedrons with Na^+ to produce hydration products (N-A-S-H) (Granizo et al. 2014). In addition, the Na^+ from alkali activators has a vital role in charge balancing of the 3D framework of Si and Al through isomorphic substitution (Hounsi et al. 2014). This charge balancing ensured the structural stability of the cementitious material and enhanced the strength. Therefore, a maximum strength of 29.61 MPa was observed after 12% addition of alkali content in the current experiment, while the compressive strength had reduced with further addition of alkali activator possibly due to the formation of carbonate as a result of Na^+ interaction with atmospheric carbon dioxide (El Hafid and Hajjaji 2015).

(b) SiO_2/Na_2O molar ratio

In this part, five series of the SiO_2/Na_2O molar ratios (0, 0.2, 0.4, 0.6 and 0.8) were used and it can be seen in Fig. 2b. Compressive strength decreased as the molar ratio exceeded the value of 0.2. The higher content of NaOH or the lower ratio of SiO_2/Na_2O dissolved the polymeric species into monomeric and oligomeric species. Consequently, the geopolymerization process accelerated and strength enhanced (Gorhan and Kurklu 2014). In contrast, the higher molar ratio of SiO_2/Na_2O indicated that the activator solution had a higher

Table 2 Chemical compositions of CG (wt%)

SiO_2	Al_2O_3	Fe_2O_3	TiO_2	K_2O	CaO	MgO	SO_3	ZnO	PbO	CuO	CdO
59.52	36.57	1.24	1.14	0.75	0.26	0.18	0.16	0.01	N.D.	N.D.	N.D.

N.D. not detected

concentration of Na_2SiO_3 which would hinder the water evaporation and polycondensation reaction (Cheng and Chiu 2003). In addition to this, the reactivity of uncalcined CG was much lower than a thermally activated one (Huang et al. 2018; Li et al. 2010). Therefore, it was a possibility that uncalcined CG required a higher concentration of NaOH or lower SiO_2/Na_2O ratio (0.2) which could dissolve it into monomeric species in the current experiment (Fernandez et al. 2011). These results were in accordance with de Vargas et al. (2011) and Muhammad et al. (2018).

(c) L/S ratios

Water is one of the important components during the synthesis of AAM. It acts as a medium which favours the dissolution, polycondensation and gelation processes during geopolymerization (Lizcano et al. 2012). In this study, the highest strength of solidified bodies was observed when the L/S ratio was 0.25 (Fig. 2c). At this ratio, the viscosity and flowability of geopolymer paste were enough for the concerned purpose. The compressive strength decreased upon further addition of water because higher water content increased the fluidity of paste and open porosity of solidified products. This statement was also verified by Lizcano et al. (2012) and Okada et al. (2009). Additionally, high initial water content could accelerate the dissolution and hydrolysis processes and thereby hindered the final polycondensation process (Zuhua et al. 2009). Finally, strength decreased.

(d) Curing temperature

According to Fig. 2d, the compressive strength of solidified bodies increased significantly with the increase in the curing temperature. The specimens cured at 30 °C were broken upon demoulding, while samples cured at 90 °C had the highest compressive strength of 25.56 MPa. Moreover, the increase in strength was more than two-fold as the temperature increased from 75 to 90 °C. This phenomenon was in line with what Slaty et al. (2013) observed. The higher curing temperature sped up the geopolymerization reactions and increased the compressive strength (Granizo et al. 2014). In addition, it was also observed that the final strength was almost achieved within 7 days, which meant higher temperature not only improved strength but also reduced the setting time. These results are in accordance with Rovnanik (2010).

Heavy metal solidification and leaching

In this section, a potential application of CG to solidify heavy metals in MSWI FA was examined through compressive strength and leaching behaviour. Based on the experimental results in "Effects of different factors on strength", A2 sample with maximum compressive strength (31.37 MPa) was served to solidify heavy metals. But regarding water content, the water requirement increased with the addition of MSWI FA so water was adjusted until the same workability was achieved.

Effect of MSWI FA proportions on compressive strength

Solidified bodies must have an appropriate compressive strength to resist external environmental pressures. Generally, the compressive strength of the solidification/stabilization products of landfills or construction material ought to be greater than 0.35 MPa and 10 MPa, respectively. Moreover, stable solidified bodies have less leaching. Thus, the compressive strength plays an essential role in the safety evaluation of solidified bodies. Figure 3 presents the compressive strength of the MSWI FA–bearing CG–based solidified bodies (CGS).

The compressive strength of CGS specimens decreased with addition of MSWI FA in comparison with control (A2). These samples with 10% and 20% addition of MSWI FA had good mechanical strength (> 10 MPa) which could be used for both constructional and landfill purposes, while further addition (up to 60%) of MSWI FA in solidified bodies could only

Table 3 Chemical compositions of MSWI FA

Major components	Ca	O	Cl	Na	Si	K	S	Mg	Fe	Al
Mass percentage (wt%)	35.57	33.95	11.95	4.24	3.27	2.87	2.33	1.55	1.13	1.08
Trace elements	Cu	Zn	Pb	Cd						
Concentration (mg/kg)	757	6342	1687	153						

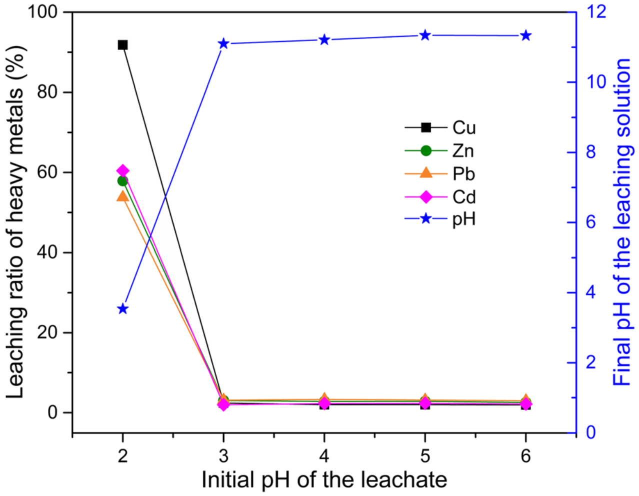

Fig. 1 Leaching ratios of heavy metals and final pH of the leaching solutions from the MSWI FA leached with acetic acid solution of different pH at an L/S ratio of 20 ml/g

be used for landfill purposes. The sudden reduction in compressive strength might be the difference in mineralogical composition, microstructures and hydration activity of CG and MSWI FA. In addition, the evaporation of extra water (a requirement for adding MSWI FA) during the preparation of specimens after being cured at 90 °C for 24 h might result in the increase of porosity in solidified products and consequently strength decreased. This finding was evidenced by Lin et al. (2009). Additionally, it was reported by Diaz-Loya et al. (2012) and Shi and Kan (2009) that the cementitious activity of MSWI FA is much lower due to a lower content of Si and Al. Hence, MSWI FA had an adverse impact on compressive strength. Meanwhile, excess calcium was detrimental to the formation of aluminosilicate network structure and substantial chloride could also influence the final performance and durability of solidified bodies (Temuujin et al. 2009; Zheng et al. 2011). Thus, the compressive strength of CGS diminished with the increase in MSWI FA amount.

Leaching experiments

The leaching solution (initial pH = 2.64 ± 0.05) of raw MSWI FA contained some heavy metals, such as Cu^{2+} (4.89 mg/L), Zn^{2+} (62.77 mg/L), Pb^{2+} (8.63 mg/L) and Cd^{2+} (1.29 mg/L). According to GB 16889-2008 standards (CN-GB 2008), Pb^{2+} and Cd^{2+} had surpassed the toxicity limits (Pb^{2+} = 0.25 mg/L and Cd^{2+} = 0.15 mg/L). Therefore, the treatment of MSWI FA via solidification/stabilization is necessary to avoid leaching of heavy metals.

Immobilization ratio and leaching concentration of each heavy metal ion varied with the addition of MSWI FA (Fig. 4). The immobilization ratios of all heavy metals were greater than 95%, which indicated that MSWI FA was effectively solidified by the CG-based geopolymer. However, the

Fig. 2 Effect of various factors on compressive strength

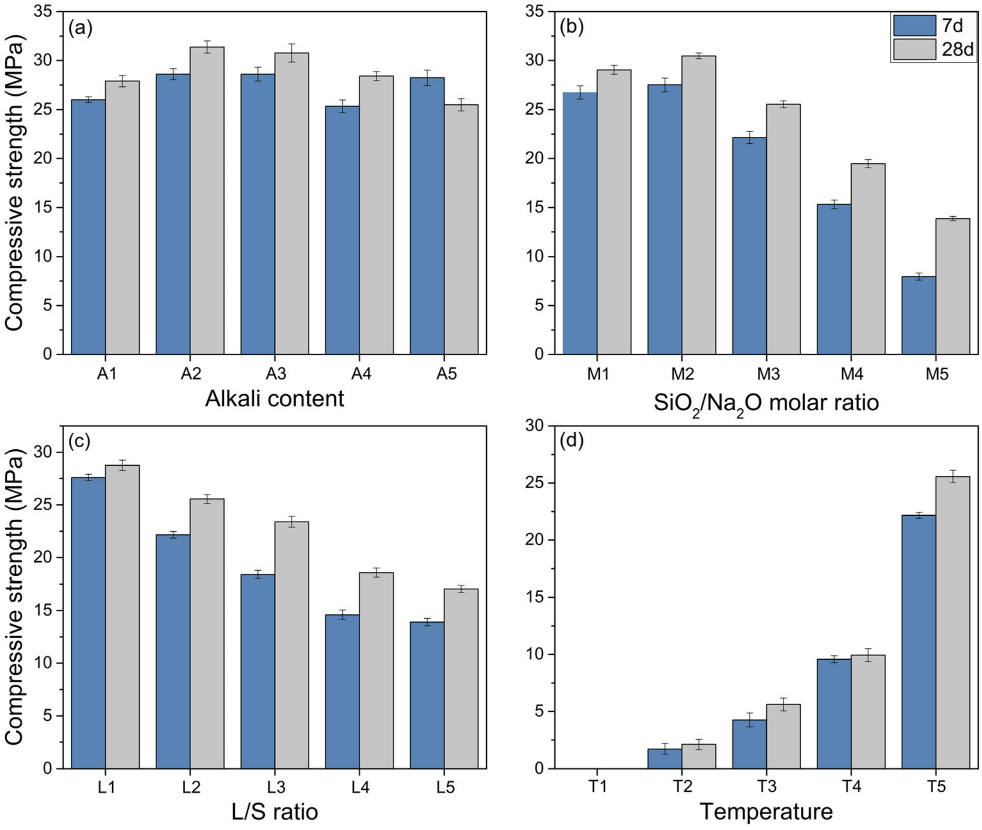

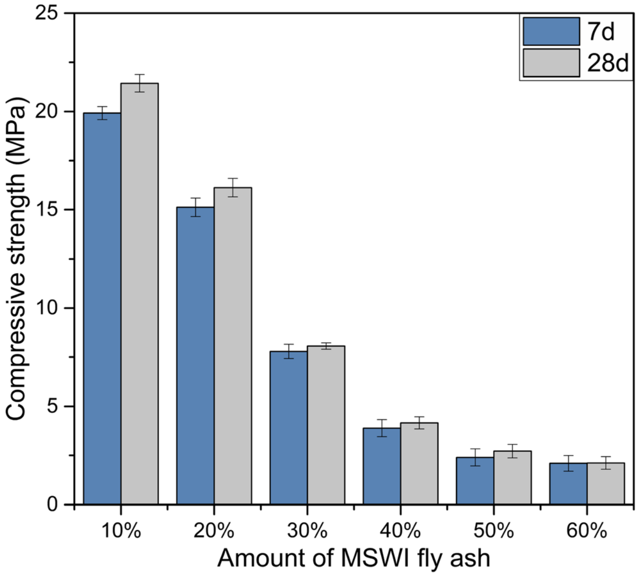

Fig. 3 The compressive strength of the CGS

increase in leaching concentrations of each heavy metal with an increment of MSWI FA was noticed. The Pb^{2+} contents in the leaching solution had crossed the critical limit upon 20% addition of MSWI FA, although the leaching concentration of Cu^{2+}, Cd^{2+} and Zn^{2+} also increased but did not surpass the safe limits. It indicated that the solidification ability of geopolymer/AAM for heavy metals is limited. The decrease in compressive strength is another reason for increasing the leaching concentration of heavy metals because the physical encapsulation ability of heavy metals decreased with the decline in compressive strength. As aforementioned, the compacted structure has higher compressive strength and lower leaching (Huang et al. 2016). Moreover, the solidified bodies having lower compressive strength could result in damage of structure and chemical bonds due to its higher exposure to leaching solution and then increase the leaching concentration. In all, the solidified bodies CGS-2 having 20% of MSWI FA could be used for both construction materials and landfill disposal.

Characterization analysis of solidified bodies

Chemical speciation transformation of heavy metals

The speciation distributions of heavy metals in the raw MSWI FA and specimen containing 50% of MSWI FA (CGS-5) cured for 28 days are shown in Fig. 5. Each metal had five chemical speciations, including exchangeable, carbonates, Fe–Mn oxides, organic matters/sulphides and residual. Compared with the former three forms, the residual fraction is unable to leach (Ye et al. 2016). The Cu^{2+}, Pb^{2+} and Cd^{2+} in raw MSWI FA existed mainly in the form of Fe–Mn oxides fraction. It is noteworthy that Cu^{2+}, Pb^{2+} and Cd^{2+} migrate to residual fraction after being solidified and their residual form contents increased up to 79.33%, 75.85% and 66.86%, respectively. This migration indicated that Cu^{2+}, Pb^{2+} and Cd^{2+} had chemically interacted with Si–O and Al–O bonds existing in geopolymer

Fig. 4 Immobilization ratios and leaching concentrations of **a** Cu^{2+}, **b** Zn^{2+}, **c** Pb^{2+} and **d** Cd^{2+}

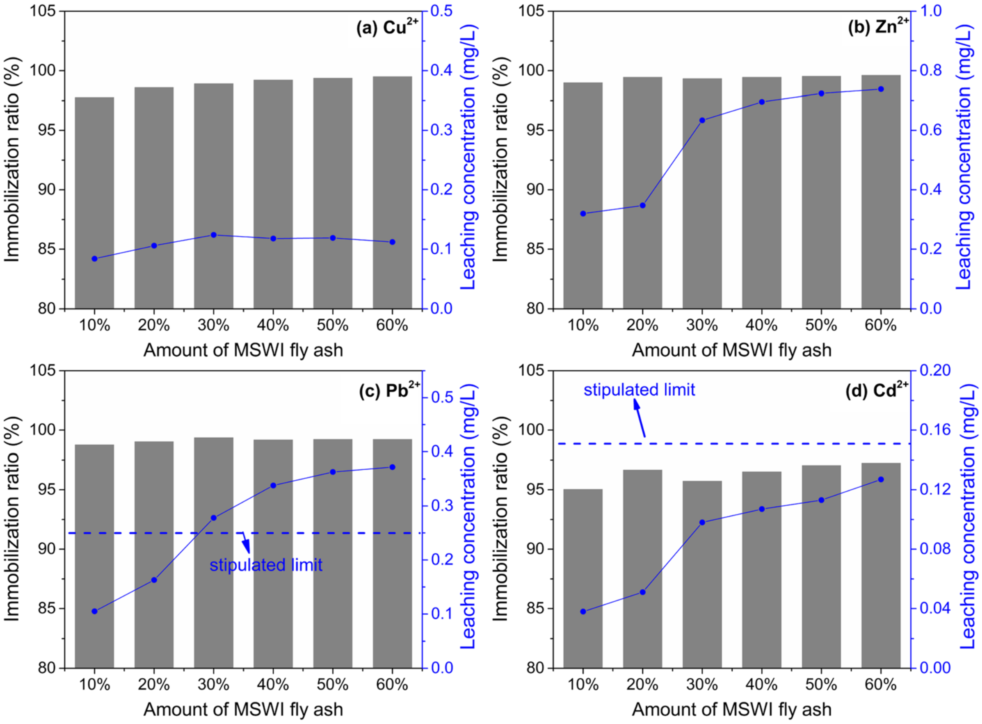

Fig. 5 Chemical speciation distributions of Cu^{2+}, Zn^{2+}, Pb^{2+} and Cd^{2+} in **a** MSWI FA and **b** CGS-5

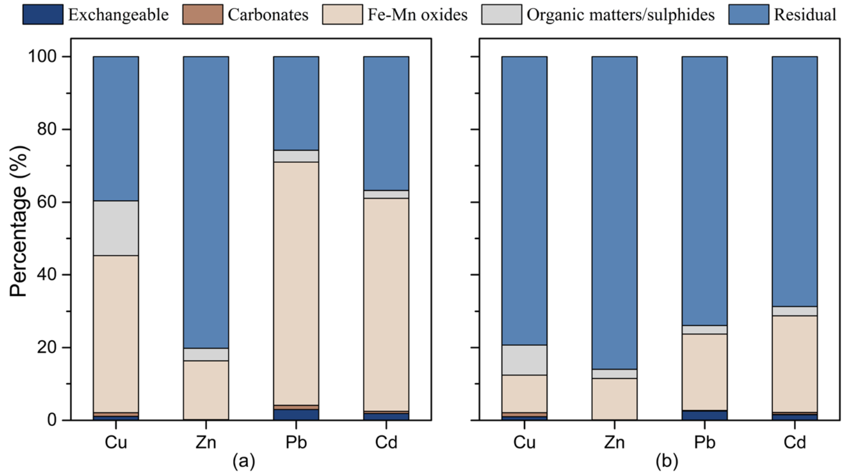

structures or trapped in structural cavities (Li et al. 2018). In this way, Cu^{2+}, Pb^{2+} and Cd^{2+} were immobilized in the geopolymer/AAM matrix and the risk of release to the environment was reduced. Regarding Zn^{2+}, the chemical speciation transformation was not significant which indicated that it might be solidified by physical encapsulation rather than chemical ways.

XRD analysis

The diffraction peaks of CG, A2, MSWI FA and CGS-5 (containing 50% MSWI) are shown in Fig. 6. There exists an amorphous phase in raw CG, but its structure is dominated by crystalline phases such as kaolinite and quartz. In the case of solidified specimens with or without MSWI FA (A2 and CGS-5), the unreacted kaolinite and quartz were observed, while the sharp reduction in number or intensities of these diffraction peaks was noticed in the presence of MSWI FA containing heavy metals. This phenomenon indicated that crystalline phases had been transformed into an amorphous phase (Wang et al. 2018b). In addition, the formation of sodalite (N-A-S-H) was observed after the addition of alkaline solution (A2). It was possible that sodium ions were integrated into the geopolymer/AAM structure, thus forming N-A-S-H (Muhammad et al. 2018; Wang et al. 2018b). However, the peaks of N-A-S-H decreased or even disappeared in the XRD pattern of CGS-5. It might be a replacement of the Na^+ ions (which acted as charge balancing in N-A-S-H) with toxic cations (e.g. Cu^{2+}, Zn^{2+},Cd^{2+} and Pb^{2+}) (Ei-Eswed et al. 2017; Zhao et al. 2004). Additionally, there were no new crystalline phases observed in CGS-5 samples. Thus, toxic heavy metal ions in MSWI FA might substitute with Na^+ into the structure of N-A-S-H and be solidified in the geopolymer/AAM structure.

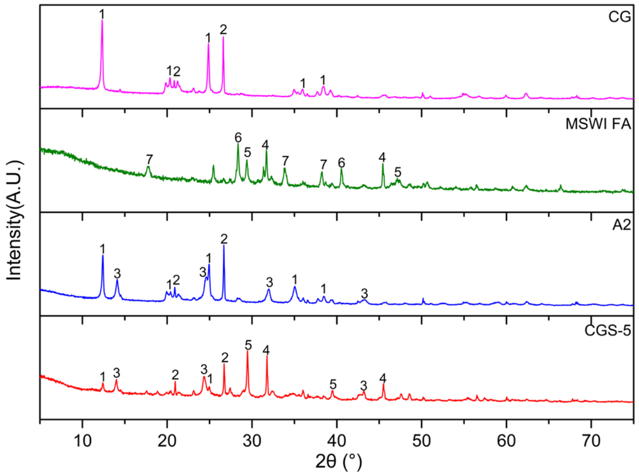

Fig. 6 The XRD patterns of the CG, A2, MSWI FA and CGS-5. 1: Kaolinite, 2: Quartz, 3: Sodalite, 4: Halite, 5: Calcite, 6: Potassium chloride and 7: CaClOH

FTIR analysis

The FTIR spectra of CG, MSWI FA, A2 and CGS-5 samples can be seen in Fig. 7. In addition, Table 4 summarizes the chemical shifts of FTIR feature bands of A2 and CGS-5 along with their corresponding species. The spectra of CG exhibited the following typical absorption peaks of kaolinite: 3619–3694 cm^{-1} (O–H stretching vibrations); 1101 cm^{-1} (Si–O plane vibrations); 914 cm^{-1} (Al–OH bending vibrations); and 540 cm^{-1} (Si–O–Al^{VI} bending vibrations) (Balczar et al. 2016; Bich et al. 2009). After the geopolymerization reaction, the intensities of these absorption peaks became weaker and even disappeared, which indicated that kaolinite in CG was dissolved with the addition of alkaline solution and this result was in accordance with the findings observed by XRD patterns of A2 and CGS-5. Asymmetric stretching vibration peak and bending vibration peak of –OH were observed at wavenumbers of around 3400 cm^{-1} and 1635 cm^{-1},

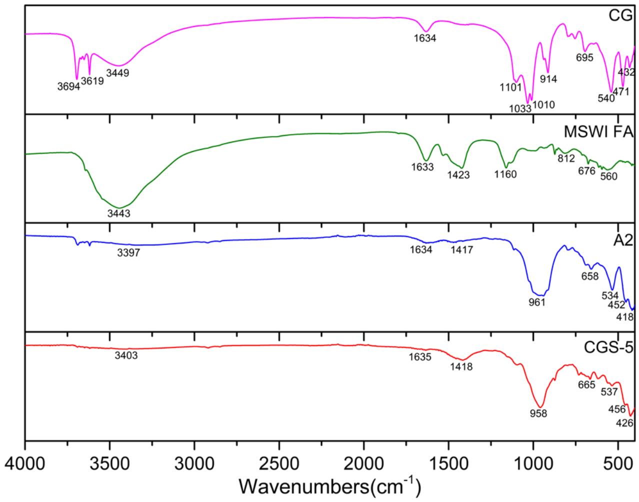

Fig. 7 The FTIR spectra of the CG, A2, MSWI FA and CGS-5

respectively, which mainly represented the presence of water molecules in these samples. The bands located at around 1420 cm^{-1} corresponded with the stretching vibration peak of O–C–O. The bands were formed by carbonates caused by reaction between alkali and CO_2 from air (Joshi et al. 2013).

Additionally, the asymmetric vibration peaks between 900 and 1000 cm^{-1} showed that the structure of the cementitious material was mainly composed of Si–O–T bonds (T = Al, Si). The Si–O–Si and O–Si–O bending vibration bands as well as Si–O–Al bending vibration bands were slightly moved towards a higher wavenumber in CGS-5 specimens. The bands at 961 cm^{-1} in A2 were due to the T–O asymmetrical stretching vibration. It was the nonbridging oxygen (T–O–Na^+) formed by the reaction of aluminosilicates and alkali (Ei-Eswed et al. 2017). Moreover, the nonbridging oxygen could give rise to the exchangeable sites which can be replaced by other heavy metal cations. It can be inferred from the above discussion that the heavy metals in the AAM/geopolymer were solidified via coordination with nonbridging oxygen (T–O^-). After addition of MSWI FA (CGS-5), this band was shifted to a lower wavenumber (958 cm^{-1}) due to toxic heavy metals ions (Zhang et al. 2008). Based on the above discussion, these heavy metals in MSWI FA could be solidified by replacing Na^+ into the geopolymer/AAM structure.

SEM analysis

The presence of irregularly shaped particles in SEM images of raw CG (Fig. 8a) and MSWI FA (Fig. 8b) was examined. The EDS spectra revealed that CG was dominated with Si and Al species, whereas the MSWI FA was enriched with Ca, Na, K and Cl-containing compounds. After alkaline activation, the smooth and compacted structures could be seen in Fig. 8c. These compacted/solidified samples were dominated with Si, Al and Na species which showed that these species have rearranged themselves after the dissolution of source materials. In addition, the existence of Na has also verified the formation of N-A-S-H gels which were also observed during XRD analysis (Xu et al. 2014). The MSWI FA containing solidified bodies, i.e. CGS-5 (Fig. 8d) had more abrasions on the surface as compared to control samples (Fig. 8c). Therefore, compressive strength decreased after addition of MSWI FA. Moreover, the presence of Ca in CGS-5 originated from MSWI FA. In Fig. 8d, some smooth surfaces indicated that heavy metals were physically encapsulated, although the heavy metals were not analysed in the EDS spectrum of solidified samples; it might be because of lower content.

Mechanism analysis

It has been already discussed in "Introduction" that geopolymerization/alkaline activation process initiates with the dissolution of the source material which follows by recombination/replacement, gelation, solidification and crystallization (Juenger et al. 2011). These reactions in the current experiment are discussed in further lines. According to XRD results, the reduction in peak intensities of kaolinite and quartz (present in raw CG, Fig. 5a) indicated that CG–based cementitious materials had first dissolved into Si and Al precursors (Huang et al. 2017). On the other hand, the formation of a new phase such as sodalite (N-A-S-H) was the evidence of rearrangement, gelation and crystallization process (A2), while the solidification of MSWI FA in A2 was verified by SEM analyses which showed the formation of a smooth and compacted structure (Fig. 7d). The formation of the compacted structure also supported the physical encapsulation

Table 4 FTIR species and corresponding bands of A2 and CGS-5

Types of species	A2 (cm^{-1})	CGS-5 (cm^{-1})
–OH asymmetrical stretching vibration	3397	3403
H–O–H bending vibration	1634	1635
O–C–O asymmetrical stretching vibration	1417	1418
Si–O–Si(Al) asymmetrical stretching vibration	961	958
Si–O–Al bending vibration	658, 534	665, 537
Si–O–Si and O–Si–O bending vibration	418, 452	426, 456

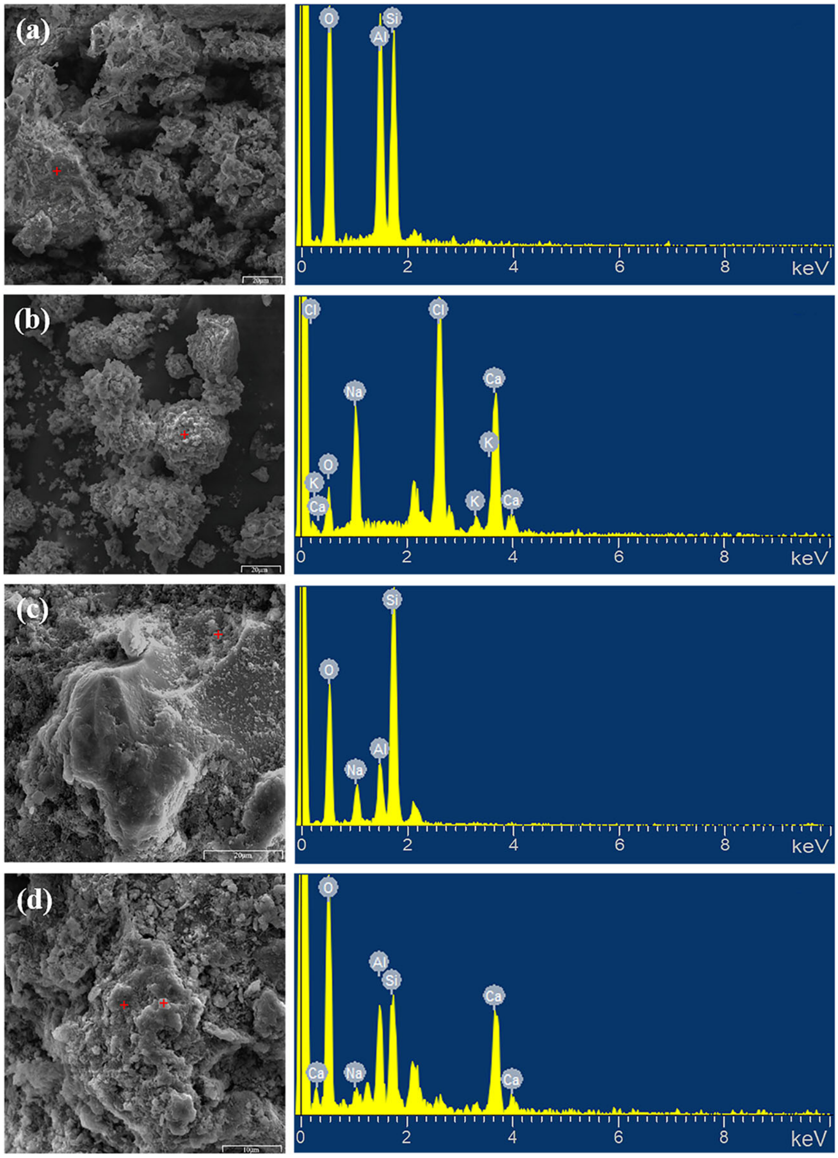

Fig. 8 The SEM images and EDS spectra of **a** CG, **b** MSWI FA, **c** A2 and **d** CGS-5

of MSWI FA. Chemical solidification of heavy metals in geopolymer/AAM structure could be analysed by their leaching properties and chemical speciation transformations (Zhang et al. 2008). Moreover, XRD and FTIR analyses showed that heavy metal ions might be solidified by replacing Na^+ ions which served as charge balancing in the geopolymeric structure. Conclusively, these heavy metals in MSWI FA were solidified in the geopolymer/AAM structure by chemical and physical ways.

Conclusions

The solidification efficiency of uncalcined CG–based cementitious materials was investigated in this study, and the following conclusions were drawn:

(1) Uncalcined CG–based cementitious materials had good mechanical properties, which were influenced by several factors (alkali contents, SiO_2/Na_2O molar ratios, L/S ratios and curing conditions). The single-factor experiment results showed that the highest compressive strength of 31.37 MPa could be achieved. The formation of N-A-S-H enhanced the compressive strength of geopolymer/AAM matrix.

(2) The geopolymer/AAM could immobilize MSWI FA and attenuate its toxicity. However, the solidification ability was limited. Increasing the amount of MSWI FA resulted in a decrease in the compressive strength of solidified bodies, thereby increasing the leaching concentration of heavy metals. The solidified bodies with a maximum of 20% addition of MSWI could be used for constructional and landfill applications.

(3) The SEM images of samples after alkaline activation showed the formation of smooth and compacted structures which meant MSWI FA was stabilized by physical encapsulation. Furthermore, the leaching behaviour, XRD, FTIR and metal speciation analyses showed that these heavy metal ions might be bounded into the 3D structure of geopolymer by interacting with chemical bonds of Si–O and Al–O or be trapped in structural cavities. By keeping these facts in view, it was concluded that uncalcined CG has potential to solidify a certain amount of hazardous waste either by physical or chemical means.

Compliance with ethical standards

Conflict of interest The authors declare that there is no conflict of interest.

Nomenclature *MSWI FA,* municipal solid waste incineration fly ash; *AAM,* alkali-activated cementitious material; *FTIR,* Fourier transform infrared spectroscopy; *CGS,* MSWI FA-bearing CG-based solidified bodies; *XRF,* X-ray fluorescence spectrometry; *EDS,* energy dispersive spectrometry; *CG,* coal gangue; *OPC,* ordinary Portland cement; *XRD,* X-ray diffraction; *L/S,* liquid-to-solid; *SEM,* scanning electron microscopy

References

Aredes FGM, Campos TMB, Machado JPB, Sakane KK, Thim GP, Brunelli DD (2015) Effect of cure temperature on the formation of metakaolinite-based geopolymer. Ceram Int 41:7302–7311

Balczar I, Korim T, Kovacs A, Mako E (2016) Mechanochemical and thermal activation of kaolin for manufacturing geopolymer mortars - comparative study. Ceram Int 42:15367–15375

Benito P, Leonelli C, Medri V, Vaccari A (2013) Geopolymers: a new and smart way for a sustainable development Preface. Appl Clay Sci 73: 1–1

Bich C, Ambroise J, Pera J (2009) Influence of degree of dehydroxylation on the pozzolanic activity of metakaolin. Appl Clay Sci 44:194–200

Bie RS, Chen P, Song XF, Ji XY (2016) Characteristics of municipal solid waste incineration fly ash with cement solidification treatment. J Energy Inst 89:704–712

Chen L, Wang L, Cho D-W, Tsang DCW, Tong L, Zhou Y, Yang J, Hu Q, Poon CS (2019) Sustainable stabilization/solidification of municipal solid waste incinerator fly ash by incorporation of green materials. J Clean Prod 222:335–343

Cheng TW, Chiu JP (2003) Fire-resistant geopolymer produced by granulated blast furnace slag. Miner Eng 16:205–210

CN-GB (2007) Identification standards for hazardous wastes-identification for extraction toxicity (GB5085.3-2007)

CN-GB (2008) Standard for pollution control on the landfill site of municipal solid waste (GB 16889–2008)

CN-HJ (2007) Solid waste-Extraction procedure for leaching toxicity-acetic acid buffer solution method (HJ/T 300-2007)

de Vargas AS, Dal Molin DCC, Vilela ACF, da Silva FJ, Pavao B, Veit H (2011) The effects of Na2O/SiO2 molar ratio, curing temperature and age on compressive strength, morphology and microstructure of alkali-activated fly ash-based geopolymers. Cem Concr Compos 33: 653–660

Deng J, Li B, Xiao Y, Ma L, Wang CP, Bin LW, Shu CM (2017) Combustion properties of coal gangue using thermogravimetry-Fourier transform infrared spectroscopy. Appl Therm Eng 116: 244–252

Diaz-Loya EI, Allouche EN, Eklund S, Joshi AR, Kupwade-Patil K (2012) Toxicity mitigation and solidification of municipal solid waste incinerator fly ash using alkaline activated coal ash. Waste Manag 32:1521–1527

Dong L (2018) Research on aluminum and iron oxide recovery from coal gangue through acid leaching. Ph.D Thesis, China University of Mining & Technology, Beijing

Du B, Li JT, Fang W, Liu YL, Yu SY, Li Y, Liu JG (2018) Characterization of naturally aged cement-solidified MSWI fly ash. Waste Manag 80:101–111

Ei-Eswed BI, Aldagag OM, Khalili FI (2017) Efficiency and mechanism of stabilization/solidification of Pb(II), Cd(II), Cu(II), Th(IV) and U(VI) in metakaolin based geopolymers. Appl Clay Sci 140:148–156

El Hafid K, Hajjaji M (2015) Effects of the experimental factors on the microstructure and the properties of cured alkali-activated heated clay. Appl Clay Sci 116:202–210

Fernandez R, Martirena F, Scrivener KL (2011) The origin of the pozzolanic activity of calcined clay minerals: A comparison between kaolinite, illite and montmorillonite. Cem Concr Res 41:113–122

Gao K, Lin KL, Wang D, Hwang CL, Shiu HS, Chang YM, Cheng TW (2014) Effects SiO2/Na2O molar ratio on mechanical properties and the microstructure of nano-SiO2 metakaolin-based geopolymers. Constr Build Mater 53:503–510

Giasuddin HM, Sanjayan JG, Ranjith PG (2013) Strength of geopolymer cured in saline water in ambient conditions. Fuel 107:34–39

Gorhan G, Kurklu G (2014) The influence of the NaOH solution on the properties of the fly ash-based geopolymer mortar cured at different temperatures. Compos Part B 58:371–377

Granizo N, Palomo A, Fernandez-Jimenez A (2014) Effect of temperature and alkaline concentration on metakaolin leaching kinetics. Ceram Int 40:8975–8985

Hounsi AD, Lecomte-Nana G, Djeteli G, Blanchart P, Alowanou D, Kpelou P, Napo K, Tchangbedji G, Praisler M (2014) How does Na, K alkali metal concentration change the early age structural characteristic of kaolin-based geopolymers. Ceram Int 40:8953–8962

Hu W, Nie QK, Huang BS, Shu X, He Q (2018) Mechanical and microstructural characterization of geopolymers derived from red mud and fly ashes. J Clean Prod 186:799–806

Huang X, Huang T, Li S, Muhammad F, Xu GJ, Zhao ZQ, Yu L, Yan YJ, Li DW, Jiao B (2016) Immobilization of chromite ore processing residue with alkali-activated blast furnace slag-based geopolymer. Ceram Int 42:9538–9549

Huang X, Zhuang RL, Muhammad F, Yu L, Shiau YC, Li DW (2017) Solidification/stabilization of chromite ore processing residue using alkali-activated composite cementitious materials. Chemosphere 168:300–308

Huang GD, Ji YS, Li J, Hou ZH, Dong ZC (2018) Improving strength of calcinated coal gangue geopolymer mortars via increasing calcium content. Constr Build Mater 166:760–768

Istuque DB, Soriano L, Akasaki JL, Melges JLP, Borrachero MV, Monzo J, Paya J, Tashima MM (2019) Effect of sewage sludge ash on mechanical and microstructural properties of geopolymers based on metakaolin. Constr Build Mater 203:95–103

Joshi S, Kalyanasundaram S, Balasubramanian V (2013) Quantitative Analysis of Sodium Carbonate and Sodium Bicarbonate in Solid Mixtures Using Fourier Transform Infrared Spectroscopy (FT-IR). Appl Spectrosc 67:841–845

Juenger MCG, Winnefeld F, Provis JL, Ideker JH (2011) Advances in alternative cementitious binders. Cem Concr Res 41:1232–1243

Komnitsas K, Zaharaki D, Vlachou A, Bartzas G, Galetakis M (2015) Effect of synthesis parameters on the quality of construction and demolition wastes (CDW) geopolymers. Adv Powder Technol 26: 368–376

Kumar V, Kumar A, Prasad B (2019) Mechanical behavior of non-silicate based alkali-activated ground granulated blast furnace slag. Constr Build Mater 198:494–500

Lee S, van Riessen A, Chon CM, Kang NH, Jou HT, Kim YJ (2016) Impact of activator type on the immobilisation of lead in fly ash-based geopolymer. J Hazard Mater 305:59–66

Li C, Wan JH, Sun HH, Li LT (2010) Investigation on the activation of coal gangue by a new compound method. J Hazard Mater 179:515–520

Li S, Huang X, Muhammad F, Yu L, Xia M, Zhao J, Jiao BQ, Shiau Y, Li DW (2018) Waste solidification/stabilization of lead-zinc slag by utilizing fly ash based geopolymers. RSC Adv 8(32):956–32,965

Lin KL, Lin DF, Chao SJ (2009) Effects of municipal solid waste incinerator fly ash slag on the strength and porosity of slag-blended cement pastes. Environ Eng Sci 26:1081–1086

Liu XM, Zhang N, Yao Y, Sun HH, Feng H (2013) Micro-structural characterization of the hydration products of bauxite-calcination-method red mud-coal gangue based cementitious materials. J Hazard Mater 262:428–438

Lizcano M, Gonzalez A, Basu S, Lozano K, Radovic M (2012) Effects of water content and chemical composition on structural properties of alkaline activated metakaolin-based geopolymers. J Am Ceram Soc 95:2169–2177

Moukannaa S, Nazari A, Bagheri A, Loutou M, Sanjayan JG, Hakkou R (2019) Alkaline fused phosphate mine tailings for geopolymer mortar synthesis: thermal stability, mechanical and microstructural properties. J Non-Cryst Solids 511:76–85

Muhammad F, Huang X, Li S, Xia M, Zhang ML, Liu Q, Hassan MAS, Jiao BQ, Yu L, Li DW (2018) Strength evaluation by using polycarboxylate superplasticizer and solidification efficiency of Cr^{6+}, Pb^{2+} and Cd^{2+} in composite based geopolymer. J Clean Prod 188:807–815

Okada K, Ooyama A, Isobe T, Kameshima Y, Nakajima A, MacKenzie KJD (2009) Water retention properties of porous geopolymers for use in cooling applications. J Eur Ceram Soc 29:1917–1923

Pelisser F, Guerrino EL, Menger M, Michel MD, Labrincha JA (2013) Micromechanical characterization of metakaolin-based geopolymers. Constr Build Mater 49:547–553

Pereira CF, Luna Y, Querol X, Antenucci D, Vale J (2009) Waste stabilization/solidification of an electric arc furnace dust using fly ash-based geopolymers. Fuel 88:1185–1193

Reig L, Tashima MM, Soriano L, Borrachero MV, Monzo J, Paya J (2013) Alkaline activation of ceramic waste materials. Waste Biomass Valoriz 4:729–736

Rovnanik P (2010) Effect of curing temperature on the development of hard structure of metakaolin-based geopolymer. Constr Build Mater 24:1176–1183

Santa RAAB, Soares C, Riella HG (2016) Geopolymers with a high percentage of bottom ash for solidification/immobilization of different toxic metals. J Hazard Mater 318:145–153

Shi HS, Kan LL (2009) Characteristics of municipal solid wastes incineration (MSWI) fly ash-cement matrices and effect of mineral admixtures on composite system. Constr Build Mater 23:2160–2166

Slaty F, Khoury H, Wastiels J, Rahier H (2013) Characterization of alkali activated kaolinitic clay. Appl Clay Sci 75–76:120–125

Temuujin J, van Riessen A, Williams R (2009) Influence of calcium compounds on the mechanical properties of fly ash geopolymer pastes. J Hazard Mater 167:82–88

Tessier A, Campbell PGC, Bisson M (1979) Sequential extraction procedure for the speciation of particulate trace-metals. Anal Chem 51: 844–851

Wang L, Yu KQ, Li JS, Tsang DCW, Poon CS, Yoo JC, Baek K, Ding SM, Hou DY, Dai JG (2018a) Low-carbon and low-alkalinity stabilization/solidification of high-Pb contaminated soil. Chem Eng J 351:418–427

Wang YG, Han FL, Mu JQ (2018b) Solidification/stabilization mechanism of Pb(II), Cd(II), Mn(II) and Cr(III) in fly ash based geopolymers. Constr Build Mater 160:818–827

Wang L, Chen L, Cho DW, Tsang DCW, Yang J, Hou D, Baek K, Kua HW, Poon CS (2019a) Novel synergy of Si-rich minerals and reactive MgO for stabilisation/solidification of contaminated sediment. J Hazard Mater 365:695–706

Wang L, Cho DW, Tsang DCW, Cao XD, Hou DY, Shen ZT, Alessi DS, Ok YS, Poon CS (2019b) Green remediation of As and Pb contaminated soil using cement-free clay-based stabilization/solidification. Environ Int 126:336–345

Xu H, Gong WL, Syltebo L, Izzo K, Lutze W, Pegg IL (2014) Effect of blast furnace slag grades on fly ash based geopolymer waste forms. Fuel 133:332–340

Ye N, Chen Y, Yang JK, Liang S, Hu Y, Xiao B, Huang QF, Shi YF, Hu JP, Wu X (2016) Co-disposal of MSWI fly ash and Bayer red mud using an one-part geopolymeric system. J Hazard Mater 318:70–78

Yue Y, Liu ZY, Liu ZZ, Zhang J, Lu M, Zhou JZ, Qian GR (2019) Rapid evaluation of leaching potential of heavy metals from municipal solid waste incineration fly ash. J Environ Manag 238:144–152

Zhan XY, Wang LA, Hu CC, Gong J, Xu TT, Li JX, Yang L, Bai JS, Zhong S (2018) Co-disposal of MSWI fly ash and electrolytic manganese residue based on geopolymeric system. Waste Manag 82:62–70

Zhang JG, Provis JL, Feng DW, van Deventer JSJ (2008) Geopolymers for immobilization of Cr6+, Cd2+, and Pb2+. J Hazard Mater 157: 587–598

Zhang N, Liu XM, Sun HH, Li LT (2011) Pozzolanic behaviour of compound-activated red mud-coal gangue mixture. Cem Concr Res 41:270–278

Zhao HT, Deng YJ, Harsh JB, Flury M, Boyle JS (2004) Alteration of kaolinite to cancrinite and sodalite by simulated Hanford tank waste and its impact on cesium retention. Clay Clay Miner 52:1–13

Zheng L, Wang CW, Wang W, Shi YC, Gao XB (2011) Immobilization of MSWI fly ash through geopolymerization: Effects of water-wash. Waste Manag 31:311–317

Zuhua Z, Mao Y, Huajun Z, Yue C (2009) Role of water in the synthesis of calcined kaolin-based geopolymer. Appl Clay Sci 43:218–223